Thermochimica Acta, 147 (1989) 127–138
Elsevier Science Publishers B.V., Amsterdam – Printed in The Netherlands

DEHYDRATION MECHANISM OF BOUND WATER IN SEPIOLITE

T. KIYOHIRO and R. OTSUKA

Department of Mineral Resources Engineering, School of Science and Engineering, Waseda University, 4-1, Okubo 3 Chome, Shinjuku-ku, Tokyo, 169 (Japan)

(Received 16 November 1988)

ABSTRACT

The bound water dehydration of sepiolite was studied by high temperature X-ray diffractometry, thermogravimetry under controlled water vapour pressure and kinetic analysis of TG curves. The results show that the uniform folding of sepiolite crystals occurs when about 50% of the bound water is lost, entrapping the rest in the crystals. Before the folding, the dehydration rate is controlled by the water separation process from the magnesium atoms at the edges of channels, while, after the folding the rate is determined by the water diffusion process in the folded channels. Kinetic evaluation of TG curves yields an activation energy of 94 kJ mol^{-1} for the Kuzuu sepiolite and 106 kJ mol^{-1} for the Eskisehir sepiolite before the folding. The energy increases to 176 kJ mol^{-1} for the Kuzuu and 170 kJ mol^{-1} for the Eskisehir after the folding. It has been confirmed that the two-step dehydration of bound water is caused by the following two factors: (1) the difference in the activation energy of dehydration between the water in the unfolded open channel and that in the folded one, and (2) the change in the rate determining process from the water separation process to the water diffusion one.

INTRODUCTION

Sepiolite is a hydrous magnesium silicate characterized by its fibrous morphology and intra-crystalline channels, having the ideal structural formula $(Si_{12})(Mg_8)O_{30}(OH)_4(OH_2)_4 8H_2O$ for the half-unit cell [1]. This mineral is known to contain three types of water molecules in different crystal chemical states; zeolitic water, bound water and structural water. The thermal dehydration of sepiolite has been studied very extensively [2–5]. Dehydration of the bound water is of most interest as sepiolite is known to dehydrate in two steps accompanied by structural change [6–8]. Various workers have attempted to explain the two-step dehydration and some mechanism models have been proposed [9–12]. These models, however, have not yet given sufficient explanation to the dehydration behaviour. A variety of methods and techniques have been employed by various investigators to reveal the overall structural transformation mechanism. Their results, however, do not totally agree with each other [13–18].

0040-6031/89/$03.50

Sepiolite owes much of its industrial application to its molecular-sized channels and large specific surface area. The channels are lost when the transformation occurs and the physio-chemical properties are also greatly affected. Hence, it is important to understand the transformation mechanism and to obtain the precise conditions necessary for the transformation.

In this paper, an attempt has been made to derive the dehydration mechanism model of sepiolite which can explain the two-step dehydration of bound water and the characteristics of the structural transformation.

MATERIALS

Four kinds of sepiolite were used for the present study. Their localities are the Akatani mine, Niigata Pref., Japan; Kuzuu, Tochigi Pref., Japan; Vallecas, Spain; and Eskisehir, Turkey. Mineralogical properties of these minerals have been reported by several authors [19–23]. The structural formulae for the dehydrated half-unit cell containing 32 oxygens are as follows: sepiolite from the Akatani mine [19], $(Si_{11.79}Al_{0.21})(Al_{0.02}Fe^{3+}_{0.23}Fe^{2+}_{0.16}Mn^{2+}_{0.55}Mg_{6.99})O_{32}$; sepiolite from Kuzuu [20], $(Si_{11.79}Al_{0.21})(Al_{0.06}Fe^{3+}_{0.01}Mg_{7.89})Ca_{0.12}O_{32}$; sepiolite from Vallecas [24], $(Si_{11.58}Al_{0.42})(Al_{0.08}Fe^{3+}_{0.06}Mg_{7.70})Ca_{0.17}K_{0.15}Na_{0.06}O_{32}$; and sepiolite from Eskisehir [23], $(Si_{11.86}Al_{0.14})(Al_{0.03}Fe^{3+}_{0.03}Mg_{7.91})Ca_{0.05}Na_{0.02}O_{32}$.

The X-ray powder patterns of these samples and their (110) peak profiles are illustrated in Figs. 1 and 2. These indicate that the degree of crystallinity

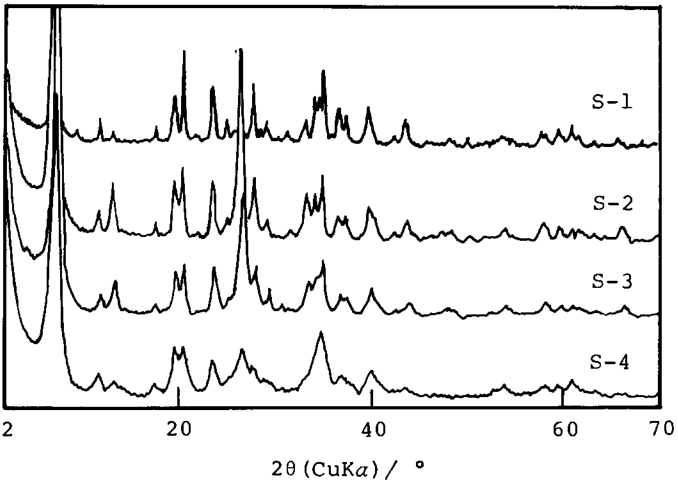

Fig. 1. X-ray diffraction patterns of sepiolites: S-1, Akatani; S-2, Kuzuu; S-3, Vallecas; and S-4, Eskisehir.

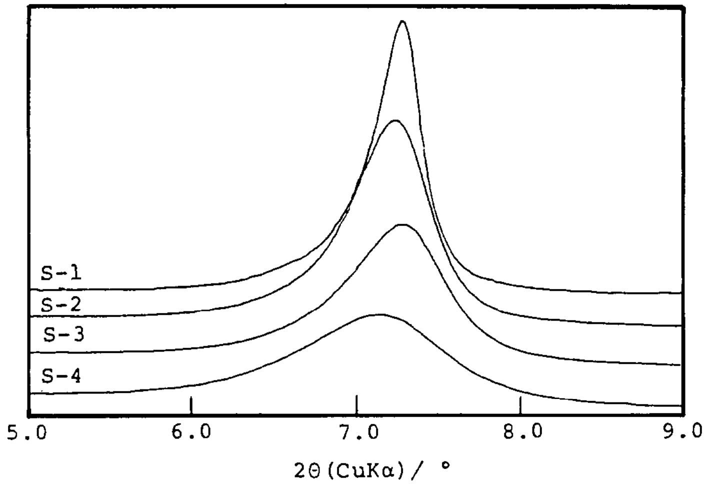

Fig. 2. (110) peak profiles of sepiolites: S-1, Akatani; S-2, Kuzuu; S-3, Vallecas; and S-4, Eskisehir.

of the samples decreases in the following sequence Akatani → Kuzuu → Vallecas → Eskisehir.

EXPERIMENTAL

High temperature X-ray diffractometry

To obtain the powder patterns of the samples at elevated temperatures, a Geigerflex (Rigaku Denki Co.) equipped with a heating unit was used. Two series of experiments were carried out to examine the change of the sepiolite (110) peak profile and the influence of water vapour pressure on the transformation temperature: (1) after recording the (110) reflection at room temperature, the sample was heated at the programmed rate of 10 °C min^{-1} up to 300 °C in static air and held for a further 120 h at that temperature. The peak profile at 300 °C was then recorded. (2) The sample was heated at the rate of 10 °C min^{-1} up to 200 °C in N_2 gas flow of 100 ml min^{-1}. It was heated further at the rate of 1 °C min^{-1} and the (110) peak intensities were recorded. The same experiment was carried out except that the N_2 gas passed through water at 30 °C before passing through the heating chamber.

Thermogravimetry under controlled water vapour pressure

The influence of water vapour pressure on the dehydration behaviour was evaluated with a simple water vapour pressure control unit, attached to a TG apparatus (TGA-30A, Shimazu Manufacturing Co.). Water evolved in a flask is led to an Allihn condenser by a carrier gas. Then, the extra water vapour condenses, giving the atmosphere in the condenser the saturated water vapour pressure. The condenser temperature is kept constant with a circulator. The water vapour is led through a teflon tube heated at about 100 ° C to the TG apparatus. Using this apparatus two series of experiments were carried out: (1) under various water vapour pressures, the sample was preheated at a temperature between 80 and 150 ° C (determined experimentally in advance) to eliminate zeolitic water. When the sample weight became constant, the recording of TG curve was started in the same atmosphere at a heating rate of 1° C min^{-1}. (2) After preheating at 50 ° C in N_2 gas flow to eliminate zeolitic water, the sample was heated at a heating rate of 1° C min^{-1}.

Kinetics

The TG curves of the Kuzuu and Eskisehir sepiolites were recorded under N_2 gas flow at the heating rates of 1, 2, 5, 10 and 20 ° C min^{-1}. The temperature at the maximum rate of dehydration were obtained by the differentiation of the TG curves. To determine the activation energy, the method of Fatemi et al. [25] was employed, using $\ln(v/T_m^2)$ versus $(1/T_m)$ plots at different heating rates. Here, v is a linear heating rate, and T_m is a temperature at the maximum rate of dehydration.

RESULTS AND DISCUSSION

High temperature X-ray diffractometry

Figure 3 shows the (110) peak profile of the Kuzuu sample at 25 ° C (a) and after heating at 300 ° C for 120 hours (b). The reflection at 7.2° (2θ, Cu $K\alpha$) is the (110) reflection of the hydrous sepiolite, while the reflection at 8.5 ° is the (110) reflection of the sepiolite anhydride. Clearly, the (110) peak intensity of the hydrous sepiolite decreases to about 2/5 of the original intensity by heating at 300 ° C for 120 hours. As the intensity of the (110) peak is known to increase about 1.5 times when the zeolitic water dehydrates [10], the actual reflecting volume of the sepiolite with unfolded structure is about 1/4 of the original volume after 120 hours of heating. Figure 4 is the superposition of the two profiles after background reduction and normalization. Obviously, the peak profile does not change even after 120 hours heating although the reflecting volume decreases to about 1/4. This fact indicates that the domain size normal to the (110) plane of the remaining unfolded sepiolite does not change in the process of transformation, which means that the structural change does not proceed in the smaller discrete zones. This also confirms the uniform transformation, at least in the

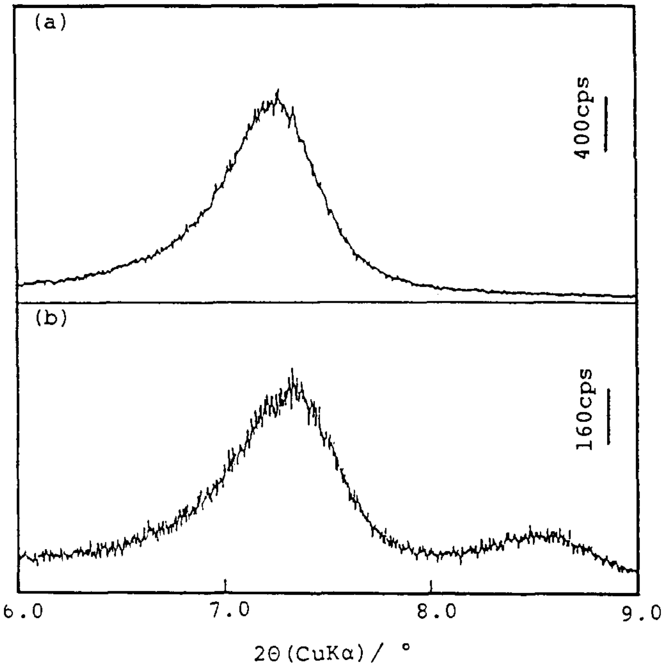

Fig. 3. (110) peak profiles of the Kuzuu sepiolite, (a) at 25 ° C, and (b) heated at 300 ° C for 120 h.

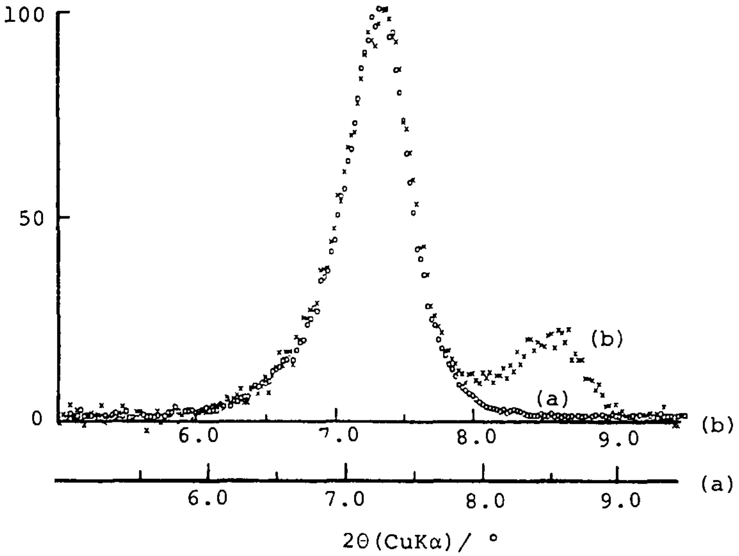

Fig. 4. Superposition of (110) peak profiles of the Kuzuu sepiolite, (a) at 25 ° C, and (b) heated at 300 ° C for 120 h after background reduction and normalization.

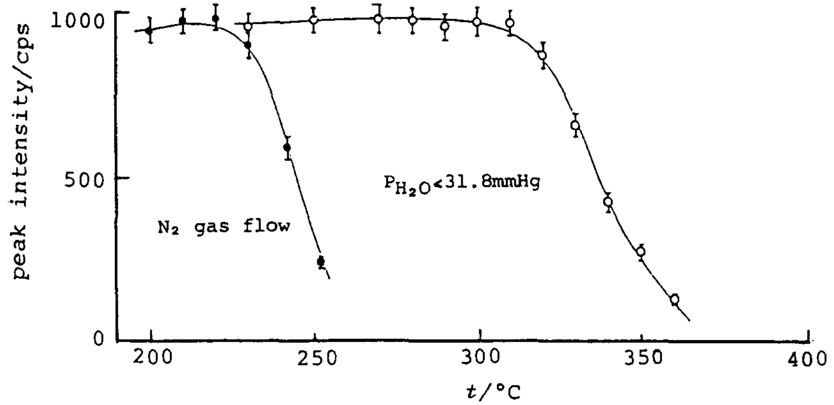

Fig. 5. The change of the (110) peak intensity of the Kuzuu sepiolite against temperature under different atmospheres.

cross-section. Thus, it is expected either that the whole crystallite transforms uniformly to anhydride structure, or that the structural change starts at the edges of the fibres and proceeds by expanding the folded region. Figure 5 shows the transformation temperature shift accompanied by the water vapour pressure change in the atmosphere. The water vapour pressure in the chamber should be lower than 31.8 mmHg, corresponding to the saturated water vapour pressure at 30 °C. This vapour pressure change shifts the transformation temperature about 100 °C higher, indicating that the transformation temperature largely depends on the water vapour pressure. This is the main reason why our observation does not agree with previous studies [13,18] with respect to the transformation temperature.

Thermogravimetry under controlled water vapour pressure

Figure 6 shows the TG curves of the Kuzuu sepiolite under various water vapour pressures. Each TG curve is normalized to make the total amount of bound water 100%. As shown in the figure, there are clear differences between the first and second steps in response to water vapour pressure variation. The first step of the dehydration is greatly influenced by water vapour pressure until completion, resulting in a 100 °C shift of the dehydration temperature at 22.3 mmHg (P_{H_2O}), while the second step hardly responds to water vapour pressure variation. This fact clearly shows the difference between the first and the second steps in the crystal chemical state of the water molecules and in the dehydration mechanism. Concerning the structural change, some previous workers assumed that the structural change was non-uniform and the channels were partially closed at the beginning of the structural change [9,10,13]. The present results, however, make it more reasonable to consider that the channels are open until the first dehydration step is completed, and then the structure changes uni-

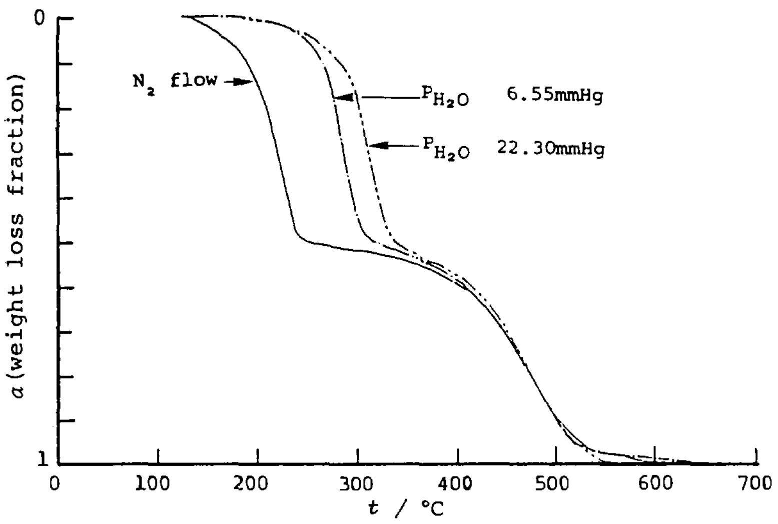

Fig. 6. TG curves of the Kuzuu sepiolite in atmospheres of various water vapour pressures.

formly. Thus, one of the two possibilities, i.e. a non-uniform structural change starting at the edges of the fibres is excluded. Furthermore, it is naturally expected that the dehydration rate is determined by the water separation process from the Mg situated at the ribbon edge of the structure. Accordingly, a dependence of the folding temperature on the water vapour pressure is expected. This has been confirmed by high temperature X-ray diffractometry.

Figure 7 shows the TG curves of the four sepiolites (Akatani, Kuzuu, Vallecas and Eskisehir). They are expressed in weight loss (%) (taking the sample weight after zeolitic water dehydration as the original weight). In contrast with the above case of water vapour pressure variation, crystallinity variation greatly affects the second dehydration step, while it does not affect the first step so much. As mentioned earlier, the Akatani sepiolite is the most crystalline and the Eskisehir the poorest. When attention is focused on the second weight-loss step of the TG curves, the Akatani takes the longest time to complete the dehydration, while the Eskisehir takes the shortest. This is best explained by considering that the water molecules diffuse out through the folded channels. The results obtained in the case of the water vapour pressure variation are in good agreement with this because the water vapour pressure cannot affect the diffusion rate. Further observation on the TG curve of the Akatani gives more evidence. In the second step, the initial rate is as high as that of the Eskisehir, while the time required to complete the dehydration is the longest. The Akatani sample used in this study is characterized as a mixture of short and long fibres. This characteristic agrees with the TG curve feature because the characteristics of short fibres dominate in the initial rate, while the long fibres lengthen the total dehydration period.

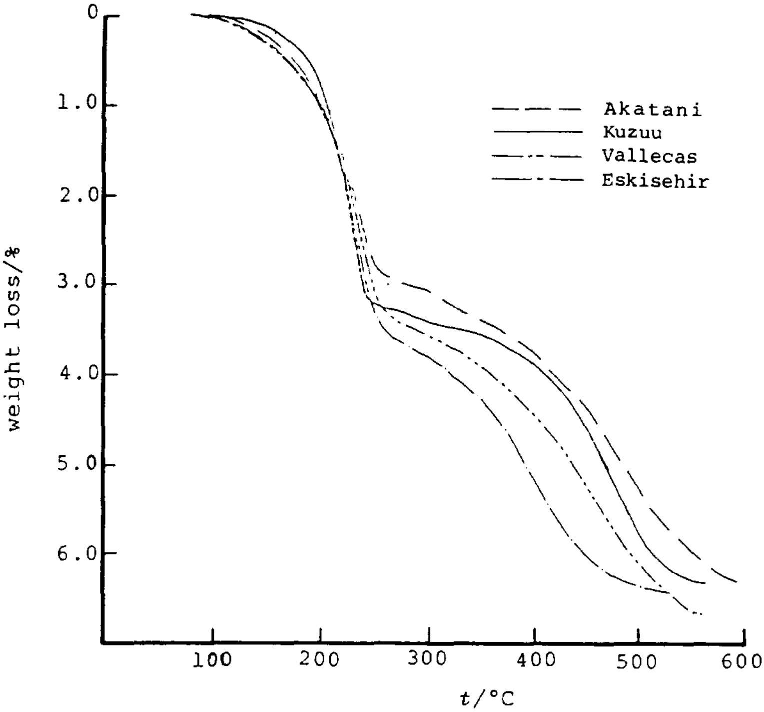

Fig. 7. TG curves of four sepiolites of different crystallinity.

Kinetics

Figure 8 shows the TG curves of the Kuzuu and the Eskisehir sepiolites at the heating rates of 1 and 20 °C $\min^{-1}$. The peak temperatures at various heating rates are listed in Table 1. The $\ln(v/T_m^2)$ versus $(1/T_m)$ plots are shown in Fig. 9. For the first step, the peak temperatures for the Kuzuu sepiolite are close to those for the Eskisehir. Thus, the plots for both samples

TABLE 1

Temperature of the maximum dehydration rate (T_m) of the first and second dehydration steps at various heating rates for the Kuzuu and Eskisehir sepiolites

Heating rate v(°C $\min^{-1}$)	T_m of the first dehydration step (°C)		T_m of the second dehydration step (°C)	
	Kuzuu	Eskisehir	Kuzuu	Eskisehir
1	228	232	468	396
2	242	249	492	407
5	265	261	512	434
10	279	276	536	446
20	294	295	550	463

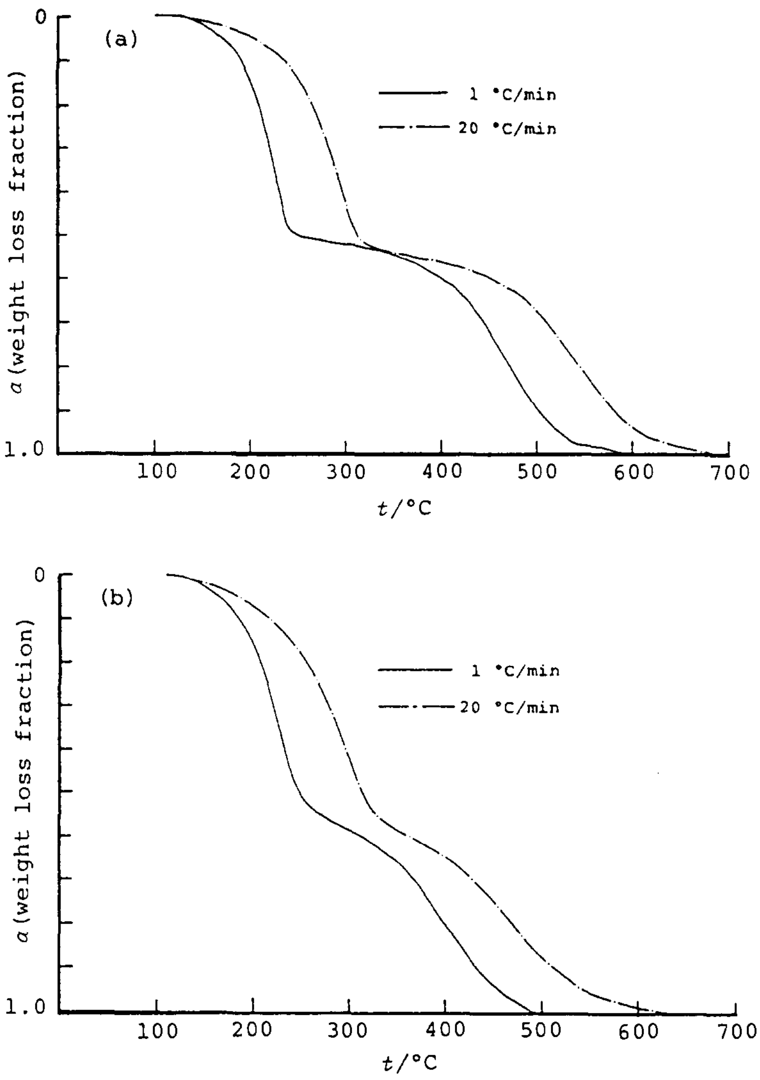

Fig. 8. (a) TG curves of the Kuzuu sepiolite under different heating rates. (b) TG curves of the Eskisehir sepiolite under different heating rates.

TABLE 2

Activation energy (E) of the first and second bound water dehydration steps for the Kuzuu and Eskisehir sepiolites

Sample	Activation energy E (kJ mol^{-1})	
	First dehydration step	Second dehydration step
Kuzuu	94	176
Eskisehir	106	170

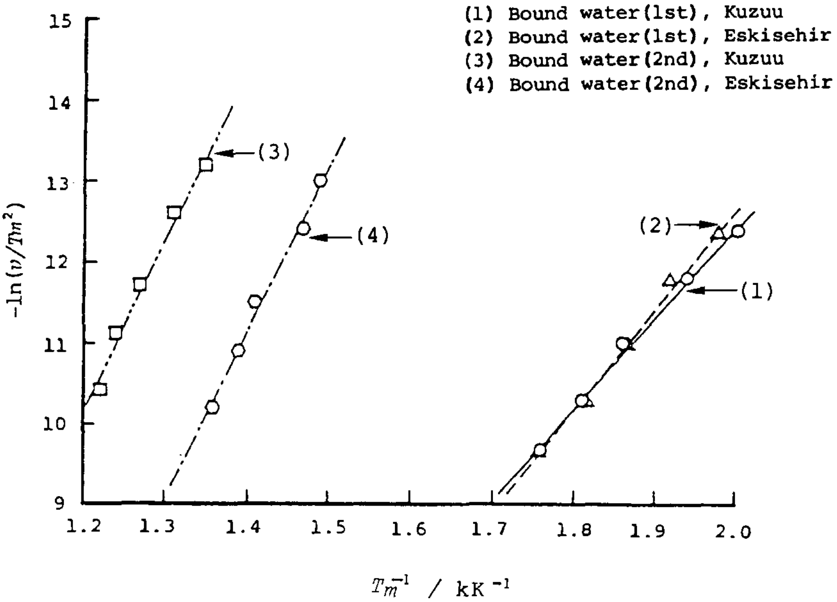

Fig. 9. $\ln(v/T_m^2)$ versus $(1/T_m)$ plots of the first and second dehydration steps of the Kuzuu and Eskisehir sepiolites.

lie almost on the same line. As for the second step, although about 80 °C difference in peak temperature is observed between the Kuzuu and the Eskisehir, the $\ln(v/T_m^2)$ versus $(1/T_m)$ plots for both samples are nearly parallel. Therefore, the activation energies of dehydration for both sepiolites are almost equal. These are listed in Table 2. This result indicates that the environment around the bound water molecules in both sepiolites is the same when they dehydrate in the second step, despite the large difference in peak temperature. Thus, the peak temperature difference is regarded as simply due to the difference in the length of folded channel, through which the water molecules diffuse out, as discussed earlier.

CONCLUSIONS

Considering the above results, the mechanism for the bound water dehydration can be summarized as follows:

(1) Bound water molecules begin to separate from the Mg at the ribbon edge and immediately come out of the crystal through the open channel. Thus, the crystal dehydrates homogeneously. The dehydration rate is determined by the water separation process from the ribbon edge.

(2) The structure becomes less stable with the progress of the bound water dehydration.

(3) When about 50% of the bound water has been lost (the first dehydration step), the structure transforms uniformly to the folded structure, which is more stable. The rest of the bound water is entrapped in the folded channels.

(4) The rest of the bound water diffuses out from the crystal through the folded channels (the second dehydration step). The dehydration rate is determined by the water diffusion process in the folded channels. Although it is still not clear whether or not the bound water is inherently distributed in two different energy levels, it is apparent that the two-step dehydration is caused by the following two factors: (i) the difference in the activation energy of dehydration between the water in the open channel and that in the folded one; and (ii) the change in the rate-determining process from the water separation process to the water diffusion one. Further study is required to solve the problem concerning the original state of the bound water.

ACKNOWLEDGEMENTS

The authors would like to thank Prof. T. Watanabe, Joetsu Univ. of Education and Dr. M. Shiraishi, National Research Institute for Pollution and Resources, for many helpful suggestions during the course of this work. This study was partly supported by the Grant in Aid for the Scientific Research of the Ministry of Education, Japan (C-6055049).

REFERENCES

1 K. Brauner and A. Preisinger, Tschermaks Miner. Petrogr. Mitt., 6 (1956) 120.
2 S. Caillère and S. Hénin, in R.C. Mackenzie (Ed.), The Differential Thermal Investigation of Clays, Mineralogical Society, London, 1957, p. 231.
3 S. Caillère and S. Hénin, in G. Brown (Ed.), The X-Ray Identification and Crystal Structures of Clay Minerals, Mineralogical Society, London, 1961, p. 325.
4 J.L. Martin-Vivaldi and P.F. Hachi-Ali, in R.C. Mackenzie (Ed.), Differential Thermal Analysis, Vol. 1, Academic Press, New York, 1970, p. 553.
5 J.L. Martin-Vivaldi and S. Robertson, in J.A. Gard (Ed.), The Electron Optical Investigation of Clays, Mineralogical Society, London, 1971, p. 255.
6 G. Kulbicki and R.E. Grim, Miner. Mag., 32 (1959) 53.
7 R. Otsuka, N. Imai and M. Nishikawa, Kogyo Kagaku Zasshi, 69 (1966) 1677 (in Japanese).
8 H. Hayashi, R. Otsuka and N. Imai, Am. Mineral., 53 (1969) 1613.
9 Y. Nathan, in L. Heller (Ed.), Proc. Int. Clay Conf., Tokyo, Vol. 1, Israel Univ. Press, Israel, 1969, p. 91.
10 R. Otsuka, H. Hayashi and N. Imai, Mem. Sch. Sci. Eng., Waseda Univ., 47 (1980) 13.
11 H. Nagata, S. Shimoda and T. Sudo, Clays Clay Miner., 22 (1974) 285.
12 M. Rautureau and C. Tchoubar, Clays Clay Miner., 24 (1976) 43.

13 Y. Nishimura, Y. Hori and H. Takahashi, Nendo Kagaku, 12 (1972) 6 (in Japanese).
14 M. Rautureau and A. Misfud, Clay Miner., 12 (1977) 309.
15 P.F. Barron and R.L. Frost, Am. Mineral., 70 (1985) 758.
16 S. Lokanatha, B.K. Mathur, B.K. Samantaray and S. Bhattacherjee, Z. Krist., 171 (1985) 69.
17 S. Lokanatha and S. Bhattacherjee, Indian J. Pure Appl. Phys., 23 (1985) 403.
18 S. Lokanatha and S. Bhattacherjee, Indian J. Pure Appl. Phys., 23 (1985) 409.
19 N. Imai, R. Otsuka and T. Nakamura, J. Jpn. Assoc. Min. Pet. Econ. Geol., 57 (1967) 39.
20 N. Imai, R. Otsuka, T. Nakamura and H. Inoue, Nendo Kagaku, 6 (1966) 30 (in Japanese).
21 S. Caillère and S. Hénin, in R.C. Mackenzie (Ed.), The Differential Thermal Investigation of Clays, Mineralogical Society, London, 1957, p. 231.
22 G.W. Brindley, Am. Mineral., 44 (1959) 495.
23 R. Otsuka, T. Mariko and T. Sakamoto, Mem. Sch. Sci. Eng., Waseda Univ., 37 (1973) 43.
24 R. Otsuka and K. Yamamoto, unpublished results (1987).
25 N.S. Fatemi, R. Whitehead, D. Price and D. Dollimore, Thermochim. Acta, 78 (1984) 437.